Room-temperature light emission from an airbridge double-heterostructure microcavity of Er-doped Si photonic crystal*

WANG Yue (王玥)**, **AN Jun-ming** (安俊明), **WU Yuan-da** (吴远大), **and HU Xiong-wei** (胡雄伟)
State Key Laboratory on Integrated Optoelectronics, Institute of Semiconductors, Chinese Academy of Sciences, Beijing 100083, China

(Received 23 October 2013; Revised 5 November 2015)

We experimentally demonstrate an efficient enhancement of luminescence from two-dimensional (2D) hexagonal photonic crystal (PC) airbridge double-heterostructure microcavity with Er-doped silicon (Si) as light emitters on silicon-on-insulator (SOI) wafer at room temperature. A single sharp resonant peak at 1 529.6 nm dominates the photoluminescence (PL) spectrum with the pumping power of 12.5 mW. The obvious red shift and the degraded quality factor (*Q*-factor) of resonant peak appear with the pumping power increasing, and the maximum measured *Q*-factor of 4 905 is achieved at the pumping power of 1.5 mW. The resonant peak is observed to shift depending on the structural parameters of PC, which indicates a possible method to control the wavelength of enhanced luminescence for Si-based light emitters based on PC microcavity.

Document code: A **Article ID:** 1673-1905(2016)01-0047-5
DOI 10.1007/s11801-016-5211-6

Numerous research efforts have been made to enhance light emission from silicon (Si) by a variety of means, including porous Si[1], Si nanocrystals[2], Ge/Si structures[3,4], Si doped with rare earth ions[5-7] and so on[8,9]. Among the materials mentioned above, Si doped with erbium (Er) ions is possible to obtain a radiative transition in the 4f shell of Er at the communication wavelength of ~1 550 nm, which is particularly suitable for high-density Si-based optoelectronic integration. Nevertheless, the light emission from Er-doped Si materials at room temperature is too weak for practical applications.

Photonic crystal (PC) microcavities have the advantages of strong light-matter interaction, selectivity of confined wavelengths, high quality factor (*Q*-factor) and small mode volume, which can enhance the on-resonance luminescence and suppress the off-resonance one through the Purcell effect greatly[10]. It has become a promising way to realize high-efficiency and ultra-low threshold Si-based light emitter at room temperature. Among several kinds of PC microcavities, the double-heterostructue microcavities based on mode-gap effect have been verified to possess the highest theoretical *Q*-factor (~10^7), which is desirable for the Purcell effect[11-13]. Previously, the luminescence of Si-based light emitters has been enhanced by some conventional PC microcavities, such as H_n cavity, L_3 cavity and so on[14-18].

In the paper, we try to enhance room-temperature light emission from Er-doped Si by PC airbridge double-heterostructure microcavity fabricated on silicon-on-insulator (SOI).

Fig.1(a) shows the schematic diagram of the two-dimensional (2D)-slab hexagonal PC double-heterostructure microcavity, which is constructed by cascading three PC waveguides (PCWs) with different radii of air-holes adjacent to width-reduced line-defect, named PCW1, PCW2 and PCW3, respectively. The radii of air-holes adjacent to PCW1, PCW2 and PCW3 are represented as r_1, r_2 and r_1, respectively. To construct the double-heterostructure microcavity based on mode-gap effect, r_2 is equal to r with the relationship of $r<r_1$, where r represents the radius of air-hole non-adjacent to the PCW. For realizing a single guided even-mode in the PC band-gap, the line-defect width w, defined as the distance between the centers of adjacent air-holes, is set to be $0.7w_0$, where $w_0=\sqrt{3}a$, is represented as the width of normal line-defect, and a represents the lattice period of PC. Due to the mode-gap effect, the photons with the specific frequency can be confined strongly in the central PCW2 microcavity region which is called photon well similar to an electron quantum well structure. Then though the Purcell effect, the on-resonance luminescence can be enhanced greatly. Numerical simulations based on plane-wave expansion (PWE) and finite difference time domain (FDTD) methods are used to design the microcavity structure, which ensures that the light with resonant wavelength of ~1.5 μm can be confined in the cavity.

* This work has been supported by the National Natural Science Foundation of China (No.61205044).
** E-mail: wy1022@semi.ac.cn

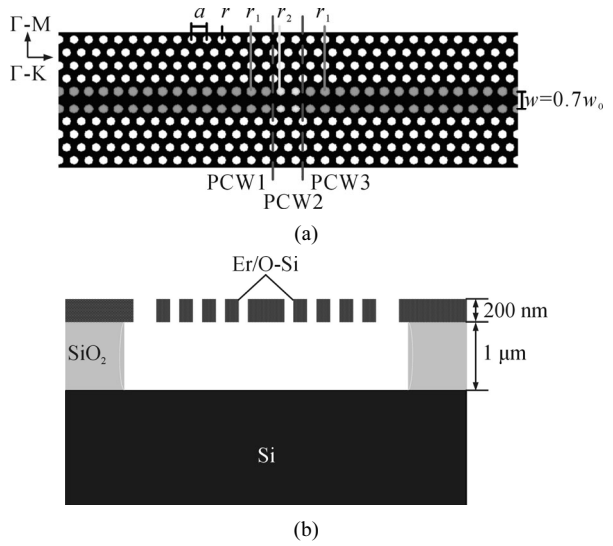

Fig.1 (a) Schematic structure diagram of PC double-heterostructure microcavity; (b) Schematic cross-sectional diagram of PC airbridge microcavity

In the experiment, the hexagonal PC structures were fabricated on SOI wafer with 200 nm-thick top Si and 1 μm-thick buried oxide (BOX). Firstly, Er ions were implanted at energy of 175 keV to a dose of 7×10^{13} cm^{-2}, and O ions were implanted at the energy of 25 keV to a dose of 4×10^{14} cm^{-2}, simultaneously, to overcome the temperature quenching of Er emission. Then, the samples were annealed at 900 °C for 30 min in N_2 atmosphere to reduce implantation damage and optically activate Er ions. We calculated the depth profiles of the implantation in the top Si layers by TRIM98 software as the approximations. The simulated results show that peak depths of Er and O ions implanted in the Si layer are 70 nm and 66 nm, respectively, and the peak concentrations of Er and O ions implanted in the Si layer are 1.59×10^{20} cm^{-3} and 6.55×10^{20} cm^{-3}, respectively. The peaks of Er and O ions locate at the same depth position approximately in the Si layer, which means that Er and O ions can form effective Er-O combinations contributed to enhance the emission of Er doped Si. Thereafter, electron beam lithography (EBL) (Raith150) was used to define the PC microcavities on the polymethyl methacrylate (PMMA) resist with depth of 220 nm, and the exposing dose was 120 μC/cm^2. Then the patterns were transferred to the top Si layer by inductively coupled plasma (ICP) (Alcatel 601E) etching using SF_6 and C_4F_8 gases with gas-flow rates of 60 cm^3/min and 65 cm^3/min, respectively, and the ICP power was 800 W. The air-holes were drilled down to the BOX layer. Moreover, to achieve a higher Q-factor, a free-standing membrane named as PC airbridge slab structure was formed by removing the supporting BOX layer using wet chemical etching by buffered oxide etching (BOE) solution, whose schematic cross-sectional diagram is shown in Fig.1(b). Fig.2(a) shows the scanning electron microscope (SEM) image of the fabricated PC double-heterostructure microcavity. The measured PC lattice period a, the radii of air-holes r_1 and r (r_2) are 435 nm, 128.3 nm and 110.5 nm, respectively. Fig.2(b) shows the SEM image of PC airbridge slab.

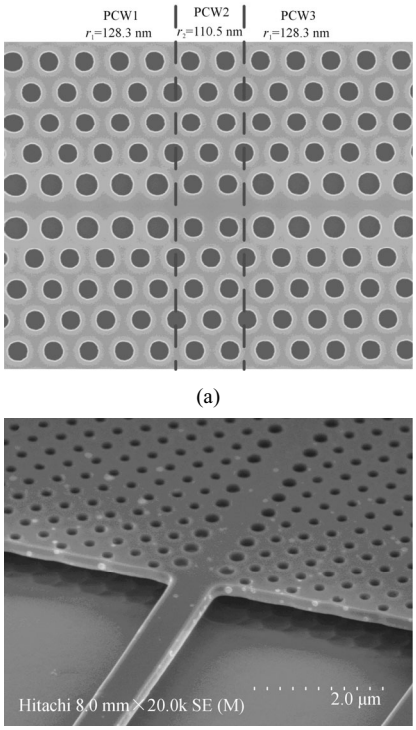

Fig.2 SEM images of (a) the fabricated PC double-heterostructure microcavity and (b) PC airbridge slab structure

The micro-photoluminescence (μ-PL) measurements were performed at room temperature (T=300 K) using micro-Raman spectroscopy (JY HR-800) equipped with an Ar^+ laser working at 488 nm, and the schematic diagram of measurement equipment is shown in Fig.3. The sample was focused and excited by the pump laser through a microscope objective lens, and the size of the spot was around 2 μm. The PL signal was collected by the same lens and recorded by a single InGaAs detector array cooled down by liquid nitrogen. Fig.4 shows the room-temperature PL spectra of the PC airbridge double-heterostructure microcavities and the unpatterned region on the same SOI wafer at the pumping power of 12.5 mW, respectively. According to the theory of microcavity, in the condition of weak coupling between the emitter and its electromagnetic surrounding, the existence of microcavity can change the spectrum distribution of the optical mode. When the spontaneous emission wavelength matches with the optical resonant wavelength, the spontaneous emission will be enhanced, otherwise, the spontaneous emission will be suppressed. Therefore, the PL intensity of Er:Si is enhanced greatly at the resonant wavelength (on-resonance), but is suppressed greatly at the other wavelengths (off-resonance). As shown in Fig.4, a single sharp resonant peak is observed at wavelengths

of 1 529.6 nm, suggesting a strong optical resonance inside the microcavity. Compared with the case of identically implanted unpatterned SOI region, the significant luminescence enhancements is achieved due to Purcell effect, and the full width at half maximum (*FWHM*) of the resonant peak is about 489 pm, from which *Q*-factor of 3 128 is deduced.

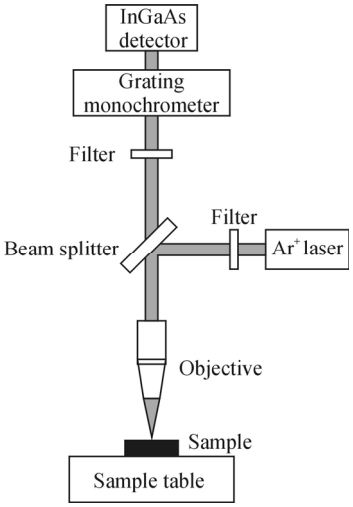

Fig.3 The schematic diagram of μ-PL measurement equipment

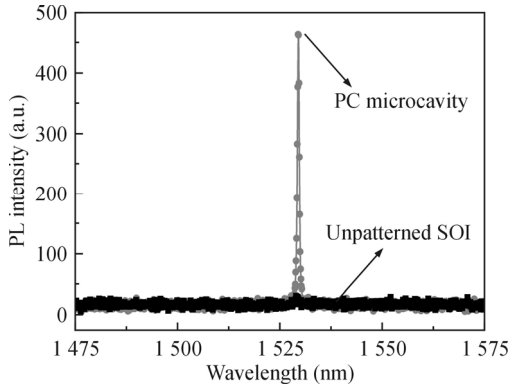

Fig.4 PL spectra of the airbridge double-heterostructure microcavities and the unpatterned SOI region at the pumping power of 12.5 mW at room temperature (*T*=300 K)

In general, PCs based on compound semiconductors undergo undesirable surface-related nonradiative recombination and show strong pumping power dependence. To investigate the pumping power dependence in the airbridge cavity, PL spectra were measured as a function of pumping power. Fig.5(a) and (b) show the evolution of the PC airbridge double-heterostructure microcavity resonance with pumping power increasing from 1.5 mW to 12.5 mW. The observed spectral red shift of the resonance with increase of power is correlated to the refractive index increase resulting from sample heating due to thermo-optic effect, and the *Q*-factor decreases with pumping power increasing due to the free-carrier absorption (FCA) of the photo-generated carriers. As the pumping power increases, the FCA increases and becomes a significant fraction of the total loss. The *Q*-factor of the cavity is decided by the intrinsic *Q*-factor Q_{int} and the *Q*-factor given by the FCA $Q_{abs}=2\pi n/\alpha\lambda$, following the equation of $1/Q=1/Q_{int}+1/Q_{abs}$, where α is the FCA coefficient, n is the refractive index, and λ is the resonant wavelength. As the pumping power increases, the change of the Q_{int} with temperature can be negligible, as a result of the small change in refractive index, and the *Q*-factor is limited by Q_{abs}. The FCA coefficient α is proportional to the density of the total free-carrier density N_{FCA}, which increases with the increase of pumping power. Therefore, Q_{abs} decreases as the pumping power increases, which means that the *Q*-factor of the cavity decreases as the pumping power increases. These results indicate that the FCA of photo-generated carriers has a big influence on the *Q*-factors of the PL peaks, and intrinsic *Q*-factors should be measured under extremely low pumping power in PL method.

Fig.5(c) shows the measured PL intensities and the magnified Lorentz fitted curve of the PL spectrum for the resonant mode of airbridge cavity at the pumping power of 1.5 mW. The wavelength of resonant mode of airbridge cavity are 1 527.1 nm, and the *FWHM* of resonant mode is about 311 pm, corresponding to the *Q*-factor of 4 905.

We also explore the possibility of performing a fine lithographic tuning of the cavity mode by changing the lattice period of the airbridge cavity during the fabrication process. Fig.6(a) shows the room-temperature PL spectra from series of microcavities with different lattice periods, which are varied from 414 nm to 435 nm, when keeping $r/a=r_2/a=0.254$ and $r_1/a=0.295$ fixed. As seen in Fig.6(a), the resonant peak moves to long wavelength side with lattice period increasing. This agreement comes from scaling law of PC structure. All the four spectra are similar because the peaks all correspond to the same cavity mode supported by the double-heterostructure microcavity. This gives clear evidence that the luminescence enhancement originates from the optical resonance by the microcavity. Fig.6(b) shows the dependence of resonant peak wavelength on PC lattice period. The curve is nearly straight line, which means that the resonant wavelength is linearly proportional to the lattice period, which provides us an efficient way to tune the wavelength of enhanced luminescence by adjusting the PC lattice period. Through carefully designing the structural parameters, we can adjust the wavelength of enhanced luminescence in a very large range.

We also explore the possibility of performing a fine lithographic tuning of the cavity mode by changing the lattice period of the airbridge cavity during the fabrication process. Fig.6(a) shows the room-temperature PL spectra from series of microcavities with different lattice periods, which are varied from 414 nm to 435 nm, when keeping $r/a=r_2/a=0.254$ and $r_1/a=0.295$ fixed. As seen in Fig.6(a), the resonant peak moves to long wavelength

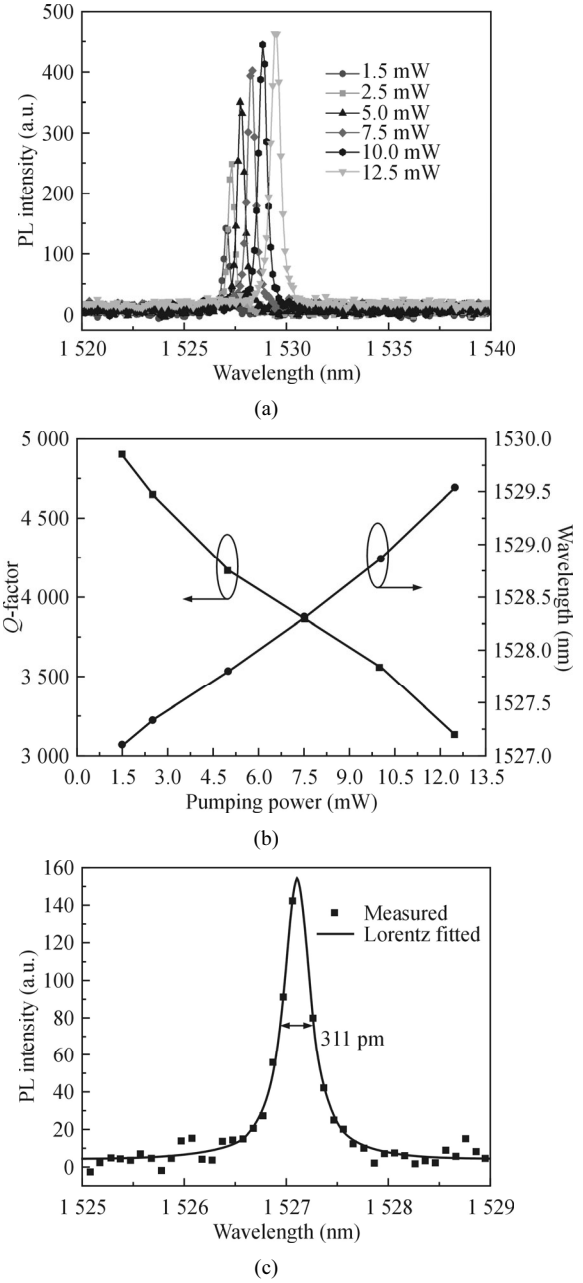

Fig.5 (a) The dependence of PL intensity of the air-bridge cavity resonance on pumping power at room temperature; (b) *Q*-factors and peak wavelengths of the resonant mode of the cavity extracted from the PL spectra at different pumping powers; (c) The magnified measured and Lorentz fitted curve of the PL spectrum for the cavity mode at the pumping power of 1.5 mW

side with lattice period increasing. This agreement comes from scaling law of PC structure. All the four spectra are similar because the peaks all correspond to the same cavity mode supported by the double-heterostructure microcavity. This gives clear evidence that the luminescence enhancement originates from the optical resonance by the microcavity. Fig.6(b) shows the dependence of resonant peak wavelength on PC lattice period. The curve is nearly straight line, which means that the resonant wavelength is linearly proportional to the lattice period, which provides us an efficient way to tune the wavelength of enhanced luminescence by adjusting the PC lattice period. Through carefully designing the structural parameters, we can adjust the wavelength of enhanced luminescence in a very large range.

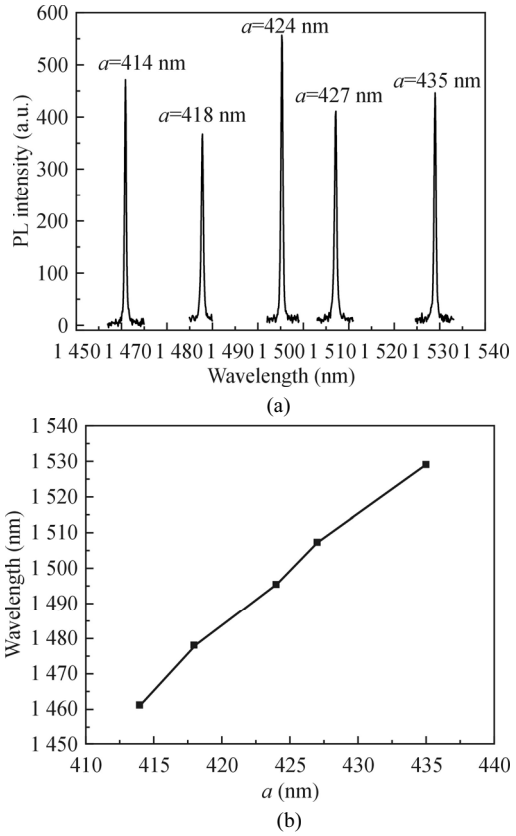

Fig.6 (a) Room-temperature PL spectra of the PC air-brdge double-heterostructure microcavities with lattice period varying from 414 nm to 435 nm at the pumping power of 10 mW; (b) The dependence of resonant peak wavelength on PC lattice period

In conclusion, we fabricate 2D-slab hexagonal PC air-bridge double-heterostructure microcavities with Er-doped Si as light emitters on SOI wafer, and significant luminescence enhancement at wavelength of ~1 530 nm is observed at room temperature. The maximum measured *Q*-factor 4 905 is achieved at low excitation power. The dependence of resonant peaks on PC structural parameters is demonstrated, which indicates a possible method to control the wavelength of enhanced luminescence for Si-based light emitters based on PC microcavity. The results prove that the combination of PC airbridge double-heterostructure microcavity and Er-doped Si is a promising way to realize high-efficiency and high-*Q*-factor Si-based light emitters operating at room temperature, which has great research and application potential in Si-based optoelectronics integration. Further improvements can be achieved by optimizing the structure, such

as better dissipation, higher collection efficiency, electrically-pumped structures and so on.

References

[1] A. G. Cullis and L. T. Canham, Nature **353**, 335 (1991).

[2] L. Pavesi, L. D. Negro, C. Mazzoleni, G. Franzo and F. Priolo, Nature **408**, 440 (2000).

[3] W. X. Hu, B. W. Cheng, C. L. Xue, H. Y. Xue, S. J. Su, A. Q. Bai, L. P. Luo, Y. D. Yu and Q. M. Wang, Applied Physics Letters **95**, 092102 (2009).

[4] X. C. Sun, J. F. Liu, L. C. Kimerling and J. Michel, Optics Letters **34**, 1198 (2009).

[5] S. Yerci, R. Li, S. O. Kucheyev, T. T. V. Buuren, S. N. Basu and L. D. Negro, IEEE Journal of Selected Topics Quantum Electronics **16**, 114 (2010).

[6] R. Li, S. Yerci, S. O. Kucheyev, T. V. Buuren and L. D. Negro, Optics Express **19**, 5379 (2011).

[7] J. Zheng, W. C. Ding, C. L. Xue, Y. H. Zuo, B. W. Cheng, J. Z. Yu, Q. M. Wang, G. L. Wang and H. Q. Guo, Journal of Luminescence **130**, 411 (2010).

[8] GAO Hong-sheng, WANG Zhen-zhen, XIE Yi-yang, GENG Zhao-xin, KAN Qiang, WANG Chun-xia, YUAN Jun and CHEN Hong-da, Journal of Optoelectronics·Laser **25**, 1338 (2014). (in Chinese)

[9] WU Lei, XIE Sheng, MAO Lu-hong, GUO Wei-lian, ZHANG Shi-lin, CUI Meng and XIE Rong, Journal of Optoelectronics·Laser **26**, 1048 (2015). (in Chinese)

[10] J. M. Gerard and B Gayral, Journal of Lightwave Technology **17**, 2089 (1999).

[11] R. Terawaki, Y. Takahashi, M. Chihara, Y. Inui and S. Noda, Optics Express **20**, 22743 (2012).

[12] H. Sekoguchi, Y. Takahashi, T. Asano and S. Noda, Optics Express **22**, 916 (2014).

[13] Z. Hu and Y. Y. Lu, Journal of Lightwave Technology **33**, 2012 (2015).

[14] A. Shakoor, R. LoSavio, S. L. Portalupi, D. Gerace, L. C. Andreani, M. Galli, T. F. Krauss and L. O'Faolain, Physica B: Condensed Matter **207**, 4027 (2012).

[15] M. Makarova, V. Sih, J. Warga, R. Li, L. D. Negro and J. Vuckovic, Applied Physics Letters **92**, 161107 (2008).

[16] J. S. Zhang, Y. Wang, Y. D. Wu, X. G. Zhang, T. Jiang, J. M. An, J. J. Li, H. J. Wang and X. W. Hu, Journal of Semiconductor **32**, 094004 (2011).

[17] X. J. Xu, S. Narusawa, T. Chiba, T. Tsuboi, J. S. Xia, N. Usami, T. Maruizumi and Y. Shiraki, IEEE Journal of Selected Topics in Quantum Electronics **18**, 1830 (2012).

[18] Y. Zhang, C. Zeng, D. P. Li, Z. Z. Huang, K. Z. Li, J. Z. Yu, J. T. Li, X. J. Xu, T. Matruizumi and J. S. Xia, IEEE Photonics Journal **5**, 4500607 (2013).